Doped Organic Crystals with High Efficiency, Color-Tunable Emission toward Laser Application

ARTICLE *in* CRYSTAL GROWTH & DESIGN · NOVEMBER 2009

Impact Factor: 4.89 · DOI: 10.1021/cg9007125

13 AUTHORS, INCLUDING:

Huan Wang
Northeast Petroleum University
28 PUBLICATIONS **526** CITATIONS
SEE PROFILE

Feng Li
Jilin University
81 PUBLICATIONS **1,574** CITATIONS
SEE PROFILE

Hui Shang
Tohoku University
8 PUBLICATIONS **86** CITATIONS
SEE PROFILE

Yuguang Ma
Chinese Academy of Sciences
312 PUBLICATIONS **6,345** CITATIONS
SEE PROFILE

DOI: 10.1021/cg9007125

CRYSTAL GROWTH & DESIGN Article

2009, Vol. 9
4945–4950

Doped Organic Crystals with High Efficiency, Color-Tunable Emission toward Laser Application

Huan Wang,[†] Feng Li,*[,†] Bingrong Gao,[‡] Zengqi Xie,[†] Suijun Liu,[†] Chunlei Wang,[†] Dehua Hu,[†] Fangzhong Shen,[†] Yuanxiang Xu,[†] Hui Shang,[†] Qidai Chen,[‡] Yuguang Ma,*[,†] and Hongbo Sun[‡]

[†]*State Key Laboratory of Supramolecular Structure and Materials, Jilin University, 2699 Qianjin Avenue, Changchun, 130012, P. R. China, and* [‡]*State Key Laboratory on Integrated Optoelectronics, College of Electronic Science and Engineering, Jilin University, 2699 Qianjin Avenue, Changchun, 130023, China*

Received June 25, 2009; Revised Manuscript Received August 24, 2009

ABSTRACT: Doping an organic crystal such as an inorganic semiconductor without having a bad influence on crystalline quality is a very difficult task because weak intermolecular interactions and lattice mismatches exist in organic condensed states. We report here the successful growth of tetracene and pentacene-doped *trans*-1,4-distyrylbenzene (*trans*-DSB) crystals with high crystalline quality, large size, and excellent optical properties. The doped concentration up to 10% can be achieved by controlling the temperature of the crystal growth zone. The first key point for the crystals with a high doping ratio is the choice of the host (*trans*-DSB) and guest (tetracene or pentacene) molecules with comparable crystal lattice structures, which ensure less lattice mismatch. The second key point is crystal growth at relative high temperatures by the physical vapor transport (PVT) method, which gives the guest molecules high kinetic energy to incorporate into the crystal lattice of the host. These doped crystals with slice shape and large size (millimeter scale) maintain ordered layer structures and crystal surface continuities, which are verified by X-ray diffraction (XRD) and atomic force microscopy (AFM) analysis. Efficient energy transfer from the host to the guest and the suppressing of the interaction among the guest molecules lead to color-tunable emission and high luminescent efficiencies (blue for undoped *trans*-DSB, $\eta = 65 \pm 4\%$; green for tetracene-doped *trans*-DSB, $\eta = 74 \pm 4\%$; red for pentacene-doped *trans*-DSB, $\eta = 28 \pm 4\%$). Steady-state and time-resolved fluorescence spectroscopy of undoped and doped crystals, and their amplified spontaneous emissions, have been investigated. These doped crystals are expected to be of interest for light-emitting transistors, diodes, and electrically pumped lasers.

Introduction

Organic single crystals constructed by π-conjugated molecules have attracted great attention in the field of organic optoelectronic materials.[1] The academic motivation for organic single crystal research is their definite structures, which provide a model to investigate the basic interactions between the molecules (supramolecular interaction), and the relationship between molecular stacking modes and optoelectronic performance (luminescence and carrier mobility).[2] Meanwhile, the superiorities of organic crystals such as high thermal stability, high ordered structure, and high carrier mobility make them attractive candidates for optoelectronic devices such as optically pumped lasers,[3] field-effect transistors,[4] electroluminescence,[5] and photovoltaic cell.[6] Optically pumped laser action has been demonstrated in a broad range of conjugated polymers and oligomers.[7] However, for the electrically driven organic lasers, there still exist many problems to be resolved. One of them is that the light-emitting diodes (LEDs) are damaged before the injected current reaches the threshold value to obtain the laser (about kA/cm^2) due to the low charge carrier mobility of the disordered amorphous materials. In the view of current injection and transport, single crystalline organic semiconductors are promising materials for electrically driven organic lasers because their inherent long-range structural ordering could effectively avoid excitons annihilations resulting in the sharp decrease of luminescence quantum efficiency under the high current densities.[8]

For the traditional organic optoelectronic polycene materials such as tetracene and pentacene, it is difficult to get high-luminescence efficiency crystals and their crystals are hardly applied in electroluminescence or lasers. As we know, doping dye molecules into certain host materials is a general method to increase the luminescent efficiency of the guest molecules for the organic amorphous materials.[9] Another merit of doping is that it can shift the emission away from the absorption region of the host to decrease the absorption loss of lasers. Thus, achieving desirable light-emission doped crystal is significant toward laser application because high carrier mobility is regarded as the inherent characteristics compared with the amorphism. Doped organic molecular crystals have been paid much attention as early as 1970s, and stimulated emissions in some systems were observed in succession.[10] Further in-depth photophysical characterizations of doped systems revealed the relationships between basic optoelectronic functions and molecular structures.[11] But most of them were based on micro- or nanocrystals due to the crystal growth method selected, in which a lack of structural definition and smaller size limited the application in optoelectronic devices. The physical vapor transport (PVT) method is the common one to obtain high-quality and large-size organic single crystal,[12] and there is almost no report about high-quality doped organic crystals with high luminescent efficiency through this method until now. This might be due to the lattice mismatch and the weak intermolecular interactions

*To whom correspondence should be addressed. Address: 2699 Qianjin Avenue, Changchun 130012 P. R. China. E-mail: ygma@jlu.edu.cn (Y.M.); lifeng01@jlu.edu.cn (F.L.). Fax: (+86) 431-85168480.

Published on Web 10/01/2009

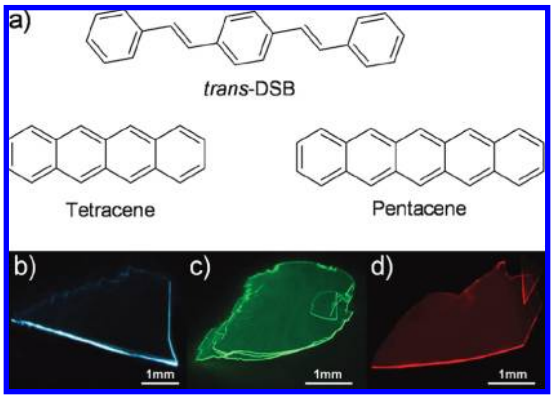

Figure 1. (a) The molecular structures of *trans*-DSB, tetracene, pentacene. (b) The pure undoped *trans*-DSB crystal. (c) Tetracene-doped *trans*-DSB crystal (tetracene/*trans*-DSB = 1:14.7 (mol ratio)). (d) Pentacene-doped *trans*-DSB crystal (pentacene/*trans*-DSB = 1:13.1 (mol ratio)) photographs under the ultraviolet lamp.

in organic crystals resulting in the difficulty of large-size doped crystal growth. In this work, based on the principle of structural comparability (including molecular structures and their stacking modes) and spectrum overlap between the host and guest (ensuring efficient energy transfer), we successfully dope a certain quantity of tetracene or pentacene (doping ratios approximate to 10%) into *trans*-1,4-distyrylbenzene (*trans*-DSB) crystal by PVT method, and maintain the structural orderings of doped crystals as proved by X-ray diffraction (XRD) and atomic force microscopy (AFM) analysis. These doped crystals have large sizes (several millimeters), high luminescent efficiency (65 ± 4% for the undoped *trans*-DSB, 74 ± 4% for the tetracene-doped *trans*-DSB, and 28 ± 4% for the pentacene-doped *trans*-DSB crystals) and color-tunable emission (blue for the undoped *trans*-DSB, green for the tetracene-doped *trans*-DSB and red for the pentacene-doped *trans*-DSB crystals). The spectra narrowings caused by amplified spontaneous emission (ASE) from the undoped *trans*-DSB, tetracene-doped *trans*-DSB and pentacene-doped *trans*-DSB crystals are observed, which show the potential application of light-emitting transistors, diodes and lasers. The molecular structures of *trans*-DSB, tetracene, and pentacene are shown in Figure 1a.

Experimental Section

UV−vis absorption and fluorescence spectra were recorded on UV-3100 and RF-5301PC spectrophotometer, respectively. Atomic force microscopy (AFM) images were recorded under ambient conditions using a Digital Instrument Multimode Nanoscope IIIa operating in the tapping mode. Si cantilever tips (TESP) with a resonance frequency of approximately 300 kHz and a spring constant of about 40 N/m were used. The wide-angle X-ray diffraction was detected with a Rigaku X-ray diffractometer (D/Max-rA, using Cu Kα radiation of wavelength 1.542 Å), and in the test the slice crystal was flatted parallel to the single-crystal Si substrate.

High performance liquid chromatography (LC-20A) was used to analyze the component content of the doped crystals. The C18 (octadecylsilyl, ODS) was used as the filling matters in column, and the column temperature was controlled as 40 °C in the test process. Ultraviolet detector (254 nm) was in response to different component. The mixed solution of CH_3OH (80%, vol.) and H_2O (20%, vol.) were used as the flow phase and the flow rate was controlled as 1 mL/min. All the detected components could be solved in tetrahydrofuran (THF).

Time-resolved fluorescence measurements were performed by the time-correlated single photon counting (TCSPC) system under right-angle sample geometry. A 379 nm picosecond diode laser (Edinburgh Instruments EPL375, repetition rate 20 MHz) was used to excite the sample. The emission was detected by a photomultiplier tube (Hamamatsu H5783p) and a TCSPC board (Becker&Hickel SPC-130). The instrument response function (IRF) is about 220 ps. All the measurements were done at room temperature (22 °C).

Crystalline state photoluminescent (PL) efficiencies were measured in an integrating sphere.[13] For the laser test, the slice crystals were irradiated by the third harmonic (355 nm) of a Nd:YAG (yttrium−aluminum−garnet) laser at a repetition rate of 10 Hz and pulse duration of about 10 ns. The energy of the pumping laser was adjusted by using the calibrated neutral density filters. The beam was focused into a stripe whose shape is adjusted to 4 × 0.5 mm through using a cylindrical lens and a slit. The edge emission of the crystals was detected using a charge-coupled-device (CCD) fiber spectrograph. All the measurements were carried out at room temperature under ambient conditions.

Tetracene and pentacene, purchased from J&K ACROS (98%), were purified by sublimation a few times before use. *trans*-DSB was synthesized and purified as referred to in our previous work.[14]

Results and Discussion

Preparation of the Crystals. The crystal growth equipment was reported in our previous work.[15] The sublimation temperatures of *trans*-DSB, tetracene, and pentacene were 220, 200, and 260 °C, respectively. The host and guest materials were chosen to be placed at the corresponding temperature zones to be heated, and the various doped crystals could be obtained under the different temperature growth zones. The detailed growth process of doped crystals was discussed and the host and guest ratios of different color-emission doped crystals were determined by chromatograph analysis in the Supporting Information. As shown in Figure 1b−d, panel b is the pure undoped *trans*-DSB crystal; panel c is the tetracene-doped *trans*-DSB crystal (tetracene/*trans*-DSB = 1: 14.7 (mol ratio)); and panel d is the pentacene-doped *trans*-DSB crystal (pentacene/*trans*-DSB = 1: 13.1 (mol ratio)). Blue, green, and red emissions from the three crystals are observed, respectively. The three crystals have the slice shape, smooth surface, and large size of several millimeters. The emissions from the edges of the crystals are stronger than that from the body surfaces, which indicates that the self-waveguided emission occurs in the crystals.

Morphology and Structure of the Crystals. Figure 2a−c shows the AFM height images at the edge areas of the *trans*-DSB, tetracene-doped *trans*-DSB, and pentacene-doped *trans*-DSB crystals. Step-like morphologies were found. From the cross-section analyses, the average heights of steps observed on the three crystal surfaces are about 1.91, 1.93, and 1.98 nm, respectively. The step heights of undoped and doped crystals are nearly similar. Figure 2d shows the diffraction patterns of wide-angle X-ray diffraction (XRD) on the slice crystals. As can be seen, the diffraction peaks occur equidistantly with varying angle degree, the baselines of the XRD patterns are straight, and the diffraction peaks are very sharp, so these slice crystals should have good ordered layer structures. The lattice parameters of *trans*-DSB were reported by Wu et al.:[16] a = 5.87 Å, b = 7.70 Å, c = 34.87 Å. Possible herringbone arrangement of *trans*-DSB molecules in the crystal was recognized in a previous work.[17] According to the Bragg equation the thicknesses of one molecular layer of *trans*-DSB, tetracene-doped *trans*-DSB, and pentacene-doped *trans*-DSB crystals are calculated to be 1.72, 1.74, and 1.75 nm, respectively, which correspond to the one-step height of these crystals in the AFM image. The values are summarized in Table 1.

Comparing the lattice constant with the XRD results, we notice that the primary diffraction spacing of *trans*-DSB

crystal is approximately identical to the monolayer height ($c/2$ = 17.43 Å) of *trans*-DSB molecules along the *ab*-plane direction, which indicates that the *ab*-plane is parallel to the crystal surface of *trans*-DSB. Also, the directions of intermolecular $\pi-\pi$ stacking of the undoped *trans*-DSB crystal and of the tetracene-doped *trans*-DSB crystal and pentacene-doped *trans*-DSB crystal are all along the *ab*-plane, based on the analysis of XRD patterns. The results of AFM morphologies and X-ray diffraction patterns suggest that all the crystals (undoped and doped) have a layer-by-layer structure and each layer corresponds to a molecular monolayer. So the structural ordering of the host *trans*-DSB crystals has been retained after doping a certain quantity of tetracene or pentacene molecules into them. Doping tetracene or pentacene into the *trans*-DSB crystal leads to a layer space a little larger, which may be due to the disturbance of the intrinsic *trans*-DSB crystal lattices caused by the embedment of doped molecules.

Structural comparability of the host and guest molecules is an important precondition for realizing the successful growth of heavy doping and large size crystal by the PVT method, which is beneficial for different intermolecular combinations in the crystal formation process and structural ordering maintenance. In our doped system, both *trans*-DSB as the host molecules and tetracene or pentacene as the guest molecules are all the linear configurations and the molecules in the crystals are arranged in similar configuration, namely, "herringbone" type structure in the *ab* plane, as proven in previous work,[16,18] where edge-to-face arene−arene interactions are much stronger than intermolecular interactions along the *c* axis direction; thus, it is easy to form layer-by-layer structures. Further, in the doped crystal formation process, host and guest molecules could freely diffuse onto the crystal surface from vapor, and then combine with neighboring molecules through intermolecular interactions to form an intact layer according to our previous work on growth characteristics of crystal prepared by PVT.[15] A certain quantity of doped guest molecules may replace the locations of original host molecules in the crystal lattice. There is hardly any report about the exact crystal structures of doped systems except for some assumptive packing models according to host molecular crystal structures.[19] In addition, we found doping uniformity is influenced by structural comparability. For example, anthracene crystal as the host and tetracene molecules as the guest could obtain the doped crystals with larger size and light emission uniformity because they belong to the polycene series and have similar stacking modes ("herringbone" type). However, doping uniformity is hard to achieve for the structural noncomparability system, such as anthracene crystal as the host and rubrene molecule (nonlinearity structure) as the doped guest. Detailed discussions of structure and spectra characteristics of tetracene or rubrene-doped anthracene crystals are shown in the Supporting Information. The emission wavelengths and quantum yields of several of these undoped and doped crystals are summarized and listed in Table 2.

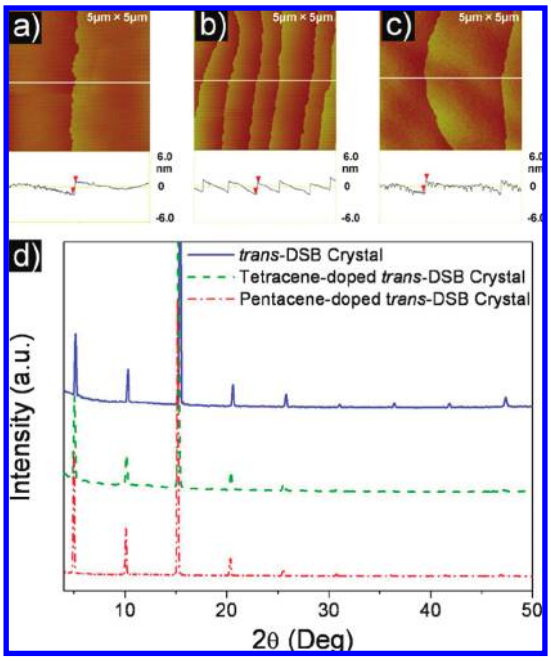

Figure 2. (a) *trans*-DSB; (b) tetracene-doped *trans*-DSB; (c) pentacene-doped *trans*-DSB slice crystal surface AFM height images. (d) XRD patterns of *trans*-DSB crystal, tetracene-doped *trans*-DSB crystal, and pentacene-doped *trans*-DSB crystal.

Optical Properties. Figure 3a shows the absorption spectra of *trans*-DSB crystal, tetracene-doped *trans*-DSB crystal, and pentacene-doped *trans*-DSB crystal. The tetracene- or pentacene-doped crystals display a similar absorption consistent with that of undoped crystal that nearly comes from host *trans*-DSB crystal. Figure 3b shows the emission spectra of *trans*-DSB crystal, tetracene-doped *trans*-DSB crystal, and pentacene-doped *trans*-DSB crystal. The PL spectra of tetracene-doped *trans*-DSB crystal show that the emission mainly comes from the tetracene molecules verifying the energy transfer. The emission peaks of tetracene molecules in the doped crystals have about 20 nm red shifts relative to that of tetracene molecules in solution, which may be caused by the conjugated effect of tetracene with the surrounding *trans*-DSB

Table 2. Summaries of the Emission Wavelengths and Quantum Yields of Some Undoped and Doped Crystals

crystal	emission wavelength (nm) 0−0	0−1	0−2	quantum yield (%)
trans-DSB	444	467	500	65 ± 4
tetracene-doped *trans*-DSB	497	531	572	74 ± 4
pentacene-doped *trans*-DSB	603	654		28 ± 4
anthracene	423	442	470	15 ± 4
tetracene-doped anthracene	494	529	570	74 ± 4
rubrene-doped anthracene	564			

Table 1. Summaries of the Molecular Layer Thicknesses and Step Heights of Undoped and Doped Crystals through XRD and AFM Analyses

crystal	*trans*-DSB	tetracene-doped *trans*-DSB	pentacene-doped *trans*-DSB
layer thickness (nm)/XRD	1.72	1.74	1.75
step height (nm)/AFM[a]	1.91 (±0.15)	1.93 (±0.15)	1.98 (±0.15)

[a] Step heights from cross-section analyses in different regions of crystal surface have slight differences and the values listed in the table are the statistic averages. The value ± 0.15 in parentheses represents the statistical zone. The calculated layer thickness corresponded well with the step height observed by AFM, but generally ~0.2 nm smaller than AFM results, due to systematic error of the instrument in the process of scanning AFM images.

molecules (The 0−1 transition emissions of tetracene solution and crystal are about 511 and 531 nm, respectively.). A similar phenomenon is also observed in the pentacene-doped *trans*-DSB crystal. The spectrum overlap of host (*trans*-DSB) crystal PL and guest (tetracene or pentacene) solution absorption is shown in Supporting Information. The herringbone arrangement of tetracene and pentacene molecules in the solid-state can quench the luminescence sharply, so their luminescent efficiencies in the aggregated state are no more than 1%. But doping tetracene or pentacene into a host crystal could effectively avoid the intermolecular aggregates. The crystalline-state PL efficiencies of the tetracene-doped *trans*-DSB and pentacene-doped *trans*-DSB crystals are as high as 74 ± 4% and 28 ± 4%, respectively. The absorption and emission separation of doped crystals will be advantageous in the lasers due to effectively decreasing the loss brought from self-absorption.

By controlling the doped content of tetracene or pentacene molecules in *trans*-DSB crystals, several crystals with different color emission are obtained, as shown in Figure S3, Supporting Information. From the photographs of these doped crystals, the emissions from the edges are stronger than those from the body surfaces, which favor an application in lasers. The PL spectra of these different color-emission crystals are also shown in Supporting Information. With the increase of the doped content of tetracene or pentacene molecules, the energy transfer from the host to the guest increases, while it induces a decrease of the host emission. It is found that the ratio of guest molecules to the host molecules is mainly influenced by the growth-zone temperature. The higher the growth-zone temperature is, the bigger the ratio of guest molecules to the host molecules is, and the worse the quality of the crystals is. This is because when the growth-zone temperature is higher, the disturbance of host-crystals lattice is more intense inducing the guest molecules to be more easily embedded into the host-crystals. The respective ratios of guest molecules to host molecules in different color emission crystals could be estimated by chromatograph analysis. For example, the mol ratios of tetracene to *trans*-DSB in the crystals shown in Figure 1c (green emission) and Figure S3a, Supporting Information (sky-blue emission) are approximately 1:14.7 and 1:33, respectively. And the mol ratios of pentacene to *trans*-DSB in the crystals shown in Figure 1d (deep-red emission) and Figure S3c (light-red emission) are approximately 1:13.1 and 1:27.8, respectively. (The details are in the Supporting Information.)

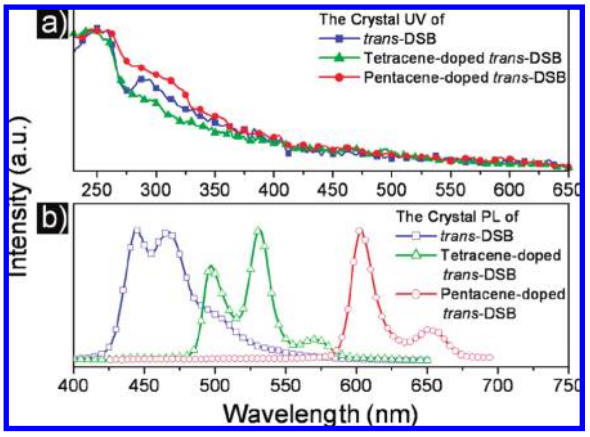

Figure 3. (a) The absorption spectra of *trans*-DSB crystal, tetracene-doped *trans*-DSB crystal, and pentacene-doped *trans*-DSB crystal. (b) The emission spectra of *trans*-DSB crystal, tetracene-doped *trans*-DSB crystal, and pentacene-doped *trans*-DSB crystal.

Time-Resolved Fluorescence. To explore the energy transfer in doped crystals, the time-resolved fluorescences of undoped and doped crystals have been investigated. Figure 4a shows the PL decay curves of undoped *trans*-DSB and tetracene-doped *trans*-DSB crystals with different mol ratios (1:33 and 1:18) monitored at the emission wavelength of 444 nm. The decay time of undoped *trans*-DSB crystal is about 3.13 ns, and that of the donor *trans*-DSB in tetracene-doped *trans*-DSB crystals decreases from 1.49 to 1.04 ns with an increase in the doping mol ratios from 1:33 to 1:18. This means efficient energy transfer exists in doped systems, and the energy transfer rate $K = 6.42 \times 10^8\ s^{-1}$ could be evaluated in tetracene-doped *trans*-DSB crystal (mol ratio (1:18)). The decay time of the acceptor tetracene in *trans*-DSB matrix is remarkably prolonged from 10.01 to 14.51 ns with an increase in the doping mol ratios from 1:33 to 1:18 monitored at the emission wavelength of 531 nm (Figure 4b). This indicates tetracene molecules are embedded in *trans*-DSB crystal with approximately uniform dispersion. Similar phenomena are found in tetracene-doped anthracene crystal (see Supporting Information). A summary of transient PL decay times for the above systems is given in Table 3.

Amplified Spontaneous Emission Experiment. Doping of organic amorphous films with dye molecules has been widely utilized to tune the emission wavelength and reduce the

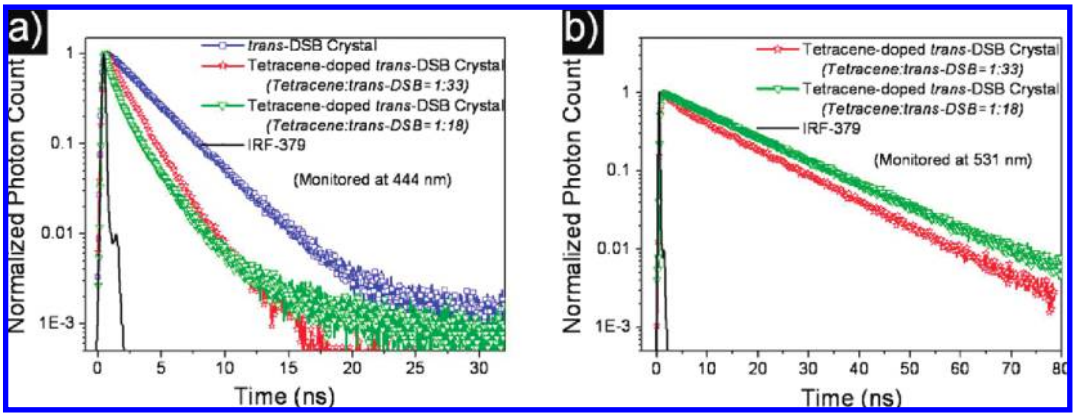

Figure 4. Time-resolved fluorescences of *trans*-DSB, tetracene-doped *trans*-DSB crystals with different mol ratios (1:33 and 1:18) at different emission wavelengths. (a) λ_{em} = 444 nm; (b) λ_{em} = 531 nm.

Table 3. Decay Data of *trans*-DSB, Anthracene, Tetracene-Doped *trans*-DSB, and Tetracene-Doped Anthracene Crystals with Different Mol Ratios

crystal	decay time τ (ns)	percentage (%)	mean lifetime τ (ns)	λ_{em} (nm)
trans-DSB	3.13	100	3.13	444 nm
tetracene-doped *trans*-DSB (1:33[a])	2.28	36.09	1.49	
	1.04	63.91		
tetracene-doped *trans*-DSB (1:18)	14.50	0.32	1.04	
	1.94	34.47		
	0.50	65.20		
tetracene-doped *trans*-DSB (1:33)	13.23	71.07	10.01	531 nm
	2.11	28.93		
tetracene-doped *trans*-DSB (1:18)	14.51	100	14.51	
anthracene	10.30	100	10.30	423 nm
tetracene-doped anthracene (1:41)	6.19	40.64	3.71	
	2.02	59.36		
tetracene-doped anthracene (1:12)	0.083	97.34	0.11	
	0.91	2.53		
	6.21	0.13		
tetracene-doped anthracene (1:41)	13.12	90.06	14.15	529 nm
	23.48	9.94		
tetracene-doped anthracene (1:12)	2.76	9.56	18.79	
	12.90	58.48		
	26.93	31.97		

[a] Mol ratios of guest to host in the parentheses are estimated by chromatograph.

lasing threshold by shifting the emission to longer wavelengths where the residual absorption is smaller.[20] Here, we realize the blue, green, and red amplified spontaneous emission (ASE) from the organic crystals by the doping method. Under the ultraviolet lamp, the emissions from the edges of all tested crystals are stronger than that from the body surface, which indicates that self-waveguided emission occurs. Waveguided propagation of the emission is thought to be one prerequisite for lasing. In the optically pumped laser experiment, the slice crystals are glued on the surface of the quartz substrates.

Because of the strong intermolecular aggregates, pure tetracene and pentacene crystals show very low luminescent efficiencies (no more than 1%), and their ASE phenomena have never been reported. The fluorescence quantum yield is not only determined by the radiative rate, but also by the emissive traps in the condensed phase. Although *trans*-DSB crystallizes in a herringbone arrangement, the quantum yield is as high as up to 65 ± 4%. This is because the *trans*-DSB crystal has low defect concentrations, as proven in previous work.[17b] However, the doped *trans*-DSB crystals with tetracene or pentacene present high luminescent efficiencies, and the ASEs from tetracene or pentacene in the doped crystals can be observed, which is mainly ascribed to suppressing of the interaction among the doped molecules. When the incident laser fluence is increased, the emission peak intensities nonlinearly grow, accompanied by the narrowing of the emission spectra, which indicates the narrowing is caused by gain- narrowing, namely, ASE. For tetracene-doped *trans*-DSB crystal, the FWHMs of the peak at 531 nm (0−1 transition) change from 18 nm at 2.4 μJ/pulse to 4 nm at 120 μJ/pulse and the threshold for the ASE is about 12 μJ/pulse from the nonlinear variation of the peak intensity with the pump energy increasing. Figure 5 shows the blue (467 nm), green (531 nm), and red (660 nm) ASEs spectra of undoped *trans*-DSB, tetracene-doped *trans*-DSB, and pentacene-doped *trans*-DSB crystals. The ASEs from the pure *trans*-DSB, tetracene-doped *trans*-DSB, and pentacene-doped *trans*-DSB crystals all occur at the emission of 0−1 transition, which suggests that the 0−1 transition has the highest gain and the self-absorption causes the relatively lower gain of 0−0 transition. The spectra narrowing and peak intensity as the function of the pumping energy, minimum fwhm, and threshold defined of undoped or doped crystals are discussed in the Supporting Information.

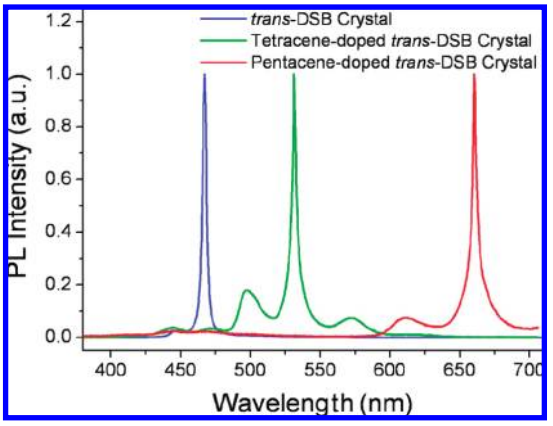

Figure 5. The ASEs spectra of undoped *trans*-DSB, tetracene-doped *trans*-DSB, and pentacene-doped *trans*-DSB crystals.

Conclusions

The PVT method is verified to get doped organic crystals effectively and several color-tunable, large-size, and high-quality doped organic crystals are obtained. The results of XRD and AFM indicate that the ordered layer structure and thin film surface continuity of the host crystals have been maintained after doping a certain quantity of tetracene or pentacene into them. The structural comparability of host and guest molecules is an important factor in the doped crystal growth, especially for the ones with a large size and heavy doping. Efficient energy transfer exists in doped crystals verified by steady-state and time-resolved fluorescence spectroscopy. Pure *trans*-DSB, tetracene- and pentacene-doped *trans*-DSB crystals show blue, green and red emission, respectively. The primary results of optically pumped laser experiments indicate that these crystals have the potential application for organic laser diodes.

Acknowledgment. We are grateful for financial support from the National Science Foundation of China (Grant Nos. 50820145304, 50733002), the Ministry of Science and Technology of China (Grant No. 2009CB623605).

Supporting Information Available: The details of doped crystals growth and characterizations, chromatograph analysis, and optically pumped laser experiments. This information is available free of charge via the Internet at http://pubs.acs.org/.

References

(1) (a) Pope, M.; Kallmann, H. P.; Mangnante, P. *J. Chem. Phys*. **1963**, *38*, 2042. (b) Avanesjan, O. S.; Benderskii, V. A.; Brikenstein, V. K.; Broude, V. L.; Korshunov, L. I.; Lavrushko, A. G.; Tartakovskii, I. I. *Mol. Cryst. Liq. Cryst*. **1974**, *29*, 165. (c) Fichou, D.; Delysee, S.; Nunzi, J. M. *Adv. Mater*. **1997**, *9*, 1178. (d) Butko, V. Y.; Chi, X.; Ramirez, A. P. *Solid State Commun*. **2003**, *128*, 431. (e) Saeki, A.; Seki, S.; Takenobu, T.; Iwasa, Y.; Tagawa, S. *Adv. Mater*. **2008**, *20*, 920.

(2) (a) Reese, C.; Bao, Z. N. *J. Mater. Chem*. **2006**, *16*, 329. (b) Mannsfeld, S. C. B.; Locklin, J.; Reese, C.; Roberts, M. E.; Lovinger, A. J.; Bao, Z. N. *Adv. Funct. Mater*. **2007**, *17*, 1617. (c) Xie, Z. Q.; Yang, B.; Cheng, G.; Liu, L. L.; He, F.; Shen, F. Z.; Ma, Y. G.; Liu, S. Y. *Chem. Mater*. **2005**, *17*, 1287. (d) Xie, Z. Q.; Yang, B.; Li, F.; Cheng, G.; Liu, L. L.; Yang, G. D.; Xu, H.; Ye, L.; Hanif, M.; Liu, S. Y.; Ma, D. G.; Ma, Y. G. *J. Am. Chem. Soc*. **2005**, *127*, 14152. (e) Xie, Z. Q.; Wang, H.; Li, F.; Xie, W. J.; Liu, L. L.; Yang, B.; Ye, L.; Ma, Y. G. *Cryst. Growth Des*. **2007**, *7*, 2512.

(3) (a) Yanagi, H.; Ohara, T.; Morikawa, T. *Adv. Mater*. **2001**, *13*, 1452. (b) Ichikawa, M.; Hibino, R.; Inoue, M.; Haritani, T.; Hotta, S.; Koyama, T.; Taniguchi, Y. *Adv. Mater*. **2003**, *15*, 213.

(4) (a) Sundar, V. C.; Zaumseil, J.; Podzorov, V.; Menard, E.; Willett, R. L.; Someya, T.; Gershenson, M. E.; Rogers, J. A. *Science* **2004**, *303*, 1644. (b) de Boer, R. W. I.; Gershenson, M. E.; Morpurgo, A. F.; Podzorov, V. *Phys. Status Solidi A* **2004**, *201*, 1302. (c) Briseno, A. L.; Mannsfeld, S. C. B.; Ling, M. M.; Liu, S.; Tseng, R. J.; Reese, C.; Roberts, M. E.; Yang, Y.; Wudl, F.; Bao, Z. N. *Nature* **2006**, *444*, 913.

(5) (a) Hisao, Y.; Takayuki, M.; Hotta, S. *Appl. Phys. Lett*. **2002**, *81*, 1512. (b) Musubu, I.; Kiyoshi, N.; Masamitsu, I.; Yoshio, T. *Appl. Phys. Lett*. **2005**, *87*, 221113. (c) Kok, W. Y.; Masaaki, Y.; Masahiro, H. *Appl. Phys. Lett*. **2006**, *88*, 083511.

(6) Tseng, R. J.; Chan, R.; Tung, V. C.; Yang, Y. *Adv. Mater*. **2008**, *20*, 435.

(7) (a) Tessler, N.; Denton, G. J.; Friend, R. H. *Nature* **1996**, *382*, 695. (b) Hide, F.; Diaz-Garcia, M.; Schwartz, B. J.; Andersson, M.; Pei, Q.; Heeger, A. J. *Science* **1996**, *273*, 1833. (c) Tessler, N. *Adv. Mater*. **1999**, *11*, 363. (d) Berggren, M.; Dodabalapur, A.; Slusher, R. E.; Bao, Z. N. *Nature* **1997**, *389*, 466. (e) Bulovic, V.; Kozlov, V. G.; Khalfin, V. B.; Forrest, S. R. *Science* **1998**, *279*, 553. (f) Moll, N.; Mahrt, R. F.; Bauer, C.; Giessen, H.; Schnabel, B.; Kley, E. B.; Scherf, U. *Appl. Phys. Lett*. **2002**, *80*, 734. (g) Reufer, M.; Riechel, S.; Lupton, J. M.; Feldmann, J.; Lemmer, U.; Schneider, D.; Benstem, T.; Dobbertin, T.; Kowalsky, W.; Gombert, A.; Forberich, K.; Wittwer, V.; Scherf, U. *Appl. Phys. Lett*. **2004**, *84*, 3262. (h) Heliotis, G.; Xia, R. D.; Turnbull, G. A.; Andrew, P.; Barnes, W. L.; Samuel, I. D. W.; Bradley, D. D. C. *Adv. Funct. Mater*. **2004**, *14*, 91.

(8) Takenobu, T.; Bisri, S. Z.; Takahashi, T.; Yahiro, M.; Adachi, C.; Iwasa1, Y. *Phys. Rev. Lett*. **2008**, *100*, 066601.

(9) Tang, C. W.; VanSlyke, S. A.; Chen, C. H. *J. Appl. Phys*. **1989**, *65*, 3610.

(10) (a) Naboikin, Y. V.; Ogurtsova, L. A.; Podgornyi, A. P.; Malkes, L. Y. *Sov. J. Quantum Electron* **1978**, *8*, 457. (b) Avanesyan, H. S.; Benderskii, V. A.; Brikenshtein, V. K.; Lavrushko, A. G.; Filippov, P. G. *Phys. Status Solidi A* **1975**, *30*, 781. (c) Schwoerer, M.; Wolf, H. C. *Organic Molecular Solids*; Wiley-VCH: New York, 2007.

(11) (a) Egelhaaf, H. -J.; Gierschner, J.; Oelkrug, D. *Synth. Met*. **2002**, *127*, 221. (b) Gierschner, J.; Egelhaaf, H. -J.; Oelkrug, D.; Müllen, K. *J. Fluoresc*. **1998**, *8*, 37. (c) Oelkrug, D.; Tompert, A.; Gierschner, J.; Egelhaaf, H. -J.; Hanack, M.; Hohloch, M.; Steinhuber, E. *J. Phys. Chem. B* **1998**, *102*, 1902. (d) Zhao, Y. S.; Fu, H. B.; Hu, F. Q.; Peng, A. D.; Yang, W. S.; Yao, J. N. *Adv. Mater*. **2008**, *20*, 79.

(12) Laudise, R. A.; Kloc, C.; Simpkins, P. G.; Siegrist, T. *J. Cryst. Growth* **1998**, *187*, 449.

(13) Kawamura, Y.; Sasabe, H.; Adachi, C. *Jpn. J. Appl. Phys. Part 1* **2004**, *43*, 7729.

(14) Xie, Z. Q.; Xie, W. J.; Li, F.; Liu, L. L.; Wang, H.; Ma, Y. G. *J. Phys. Chem. C* **2008**, *112*, 9066.

(15) Wang, H.; Xie, Z. Q.; Yang, B.; Shen, F. Z.; Li, Y. P.; Ma, Y. G. *CrystEngComm* **2008**, *10*, 1252.

(16) Wu, C. C.; Delong, M. C.; Vardeny, Z. V.; Ferraris, J. P. *Synth. Met*. **2003**, *137*, 939.

(17) (a) Spano, F. C. *Annu. Rev. Phys. Chem*. **2006**, *57*, 217. (b) Gierschner, J.; Ehni, M.; Egelhaaf, H. J.; Milián Medina, B.; Beljonne, D.; Benmansour, H.; Bazan, G. C. *J. Chem. Phys*. **2005**, *123*, 144914.

(18) (a) Cuppen, H. M.; Graswinckel, W. S.; Meekes, H. *Cryst. Growth Des*. **2004**, *4*, 1351. (b) Ruiz, R.; Choudhary, D.; Nickel, B.; Toccoli, T.; Chang, K. C.; Mayer, A. C.; Clancy, P.; Blakely, J. M.; Headrick, R. L.; Iannotta, S.; Malliaras, G. G. *Chem. Mater*. **2004**, *16*, 4497.

(19) (1) Li, H. P.; Duan, L.; Zhang, D. Q.; Dong, G. F.; Wang, L. D.; Qiu, Y. *J. Cryst. Growth* **2008**, *310*, 2537. (2) Li, H. P.; Duan, L.; Zhang, D. Q.; Dong, G. F.; Wang, L. D.; Qiu, Y. *Sci. China Ser. B-Chem* **2009**, *52*, 181. (3) Nicolet, A.; Bordat, P.; Hofmann, C.; Kol'chenko, M. A.; Kozankiewicz, B.; Brown, R.; Orrit, M. *ChemPhysChem* **2007**, *8*, 1929.

(20) McGehee, M. D.; Heeger, A. J. *Adv. Mater*. **2000**, *12*, 1655.